

# Hydrogenation of Weakly Rehybridized Ethylene on Fe(100)–H: Ethyl Group Formation

Philip B. Merrill and Robert J. Madix\*

Contribution from the Departments of Chemistry and Chemical Engineering, Stanford University, Stanford, California 94305

Received October 17, 1995<sup>⊙</sup>

**Abstract:** The bonding and reactivity of ethylene on hydrogen presaturated Fe(100) has been investigated using temperature programmed reaction spectroscopy (TPRS) and electron energy loss spectroscopy (EELS). Hydrogen preadsorbed on Fe(100) limits the extent of electron back-donation to coadsorbed ethylene, resulting in weak rehybridization relative to adsorption on clean Fe(100). Adsorption at 100 K leads to rehybridization intermediate between the  $sp^2$  gas phase species and the nearly  $sp^3$  di- $\sigma$  bound ethylene on clean Fe(100), as indicated by  $\pi\sigma$  parameters of 0.58 (0.53 for  $C_2D_4$ ). Migratory insertion of coadsorbed hydrogen into this adsorbed ethylene occurs below 170 K; vibrational spectroscopy positively identifies the intermediate formed as surface ethyl groups.

## Introduction

Previous observation of CO-promoted formation of ethane from ethylene on hydrogen-covered Fe(100) (Fe(100)–H) has prompted us to use vibrational spectroscopy to positively identify the intermediate involved. Ethylene adsorption and decomposition on clean Fe(100) has been studied extensively.<sup>1–3</sup> Ethylene adsorbs with di- $\sigma$  bonding and, upon heating, evolves  $H_2$  while forming ethynyl and methylidyne, which further decompose to evolve the remaining hydrogen, leaving carbon on the surface. Preadsorbed hydrogen inhibits the decomposition. EELS measurements demonstrate that the hydrogen adsorbs within the 4-fold hollows,<sup>4</sup> the site of decomposition proposed by Hung and Bernasek.<sup>3</sup>

Burke and Madix reported extensive temperature programmed reaction spectroscopy (TPRS) studies of the reactivity of ethylene on Fe(100)–H.<sup>1</sup> Ethylene evolves in desorption states at 150 and 225 K. These studies suggested the competitive desorption and reaction of ethylene to form adsorbed ethyl groups. Further heating of this surface results in the *reaction limited* desorption of ethylene. Since the reaction of ethylene- $h_4$  with coadsorbed deuterium showed isotopic mixing for the high temperature state to form ethylene- $d_1$ , and the kinetic isotope effect indicated that C–H(D) bond breaking is the rate limiting step liberating ethylene from this state, vinyl and vinylidene were eliminated as possible intermediates. However reactions of either ethyl or ethylidyne intermediates could be conceived to be the precursor to ethylene formation.

Three arguments were advanced against ethylidyne as the intermediate leading to ethylene formation at 225 K. First, based on the patterns observed on other metal surfaces, ethylidyne is not normally expected to form on a surface of 4-fold symmetry.<sup>5–9</sup> Second, on all surfaces where it is formed, ethylidyne decom-

poses at much higher temperatures. Third, in the presence of coadsorbed CO, this intermediate hydrogenates to evolve ethane at 165 K;<sup>10</sup> no ethane is formed without the addition of CO. Adsorbed ethyl is the intermediate most consistent with these observations.

Several features of the CO-promoted hydrogenation reaction are notable. Weakening of the Fe–H bond is readily apparent in the temperature programmed desorption of hydrogen in the presence of coadsorbed CO. Further, the rate limiting step in the evolution of ethane appears to be the formation of the intermediate when CO is coadsorbed with ethylene at 100 K. EELS measurements also demonstrate perturbation of the Fe–H bond<sup>4</sup> by coadsorbed CO and show the site conversion<sup>11</sup> of CO from atop or bridge bonding to 4-fold hollow as hydrogen vacates this site in forming both the intermediate and ethane.<sup>12</sup> The site conversion of CO appears to contribute to the driving force of the hydrogen transfer reactions.

The bonding of ethylene to the surface is undoubtedly related to its propensity for hydrogenation. Bonding of ethylene in organometallic complexes can be described by the Dewar–Chatt–Duncanson (DCD) model<sup>13,14</sup>—a combination of donation from the filled ethylene p orbitals to empty metal orbitals and donation from filled metal orbitals to unfilled ethylene  $\pi^*$  orbitals. Wong and Hoffmann have investigated the bonding of ethylene on metal surfaces by an approximate molecular orbital method (extended Hückel calculations within a tight binding formalism).<sup>15</sup> Interaction of ethylene  $\pi$  and  $\pi^*$  orbitals dominate the bonding to the surface, analogous to the DCD model. According to this treatment, antisymmetric combinations of metal s and p orbitals dominate the bonding interaction with the  $\pi$  and  $\pi^*$  orbitals of ethylene. The dominance of s and p orbitals in the bonding arises because the d orbitals (although strongly interacting) combine to form *occupied* bonding and *antibonding* states for little net bonding.

\* Corresponding author.

⊙ Abstract published in *Advance ACS Abstracts*, April 15, 1996.

(1) Burke, M. L.; Madix, R. J. *J. Am. Chem. Soc.* **1991**, *113*, 3675.

(2) Benziger, J. B.; Madix, R. J. *J. Catal.* **1980**, *65*, 49.

(3) Hung, W.-H.; Bernasek, S. *Surf. Sci.* **1995**, *339*, 272.

(4) (a) Merrill, P. B.; Madix, R. J. *Surf. Sci. in press.* (b) Merrill, P. B. Ph.D. Thesis, Stanford University, 1995; Chapter 2.

(5) Steininger, H.; Ibach, H.; Lehwald, S. *Surf. Sci.* **1982**, *117*, 685.

(6) Koel, B. E.; Bent, B. E.; Somorjai, G. A. *Surf. Sci.* **1984**, *146*, 211.

(7) Gates, J. B.; Kesmodel, L. L. *Surf. Sci.* **1983**, *124*, 68.

(8) Marinova, T. S.; Kostov, K. L. *Surf. Sci.* **1987**, *181*, 573.

(9) Hills, M. M.; Parmeter, J. E.; Mullins, C. B.; Weinberg, W. H. *J. Am. Chem. Soc.* **1986**, *108*, 3554.

(10) Burke, M. L.; Madix, R. J. *J. Am. Chem. Soc.* **1991**, *113*, 1475.

(11) Merrill, P. B.; Madix, R. J. *Surf. Sci.* **1992**, *271*, 81.

(12) EELS measurements demonstrate a decrease in atop  $\nu$ CO which correlates to an increase in 4-fold  $\nu$ CO; bridge  $\nu$ CO are prominent before and after the conversion.<sup>11</sup> However, these studies cannot distinguish between (1) direct conversion of CO from atop to 4-fold sites and (2) conversion from bridge to 4-fold sites along with simultaneous conversion from atop to bridge sites.

(13) Dewar, J. S. *Bull. Soc. Chim. France* **1951**, *18*, C71.

(14) Chatt, J.; Duncanson, L. A. *J. Chem. Soc.* **1953**, 2939.

(15) Wong, Y.-T.; Hoffmann, R. *J. Chem. Soc., Faraday Trans.* **1990**, *86*, 4083.

Vibrational spectroscopy has been utilized to determine the bonding of ethylene and its reactivity in several organometallic complexes<sup>13,14,16</sup> and on various metal surfaces,<sup>17–20</sup> demonstrating a wide variety of binding and reaction pathways. Perhaps the most straightforward method for determining the state of rehybridization of ethylene complexes, vibrational spectroscopy generally reveals a reduced C–C stretching frequency relative to gas phase ethylene. However, these shifts of  $\nu_{CC}$  are minor in comparison to the  $\nu_{CC}$  shifts for C–C bonds in  $sp^1$  C<sub>2</sub>H<sub>2(g)</sub> (1974 cm<sup>-1</sup>),  $sp^2$  C<sub>2</sub>H<sub>4(g)</sub> (1623 cm<sup>-1</sup>), and  $sp^3$  C<sub>2</sub>H<sub>6(g)</sub> (993 cm<sup>-1</sup>).<sup>21</sup> Generally, ethylene binds on metal surfaces with  $\pi$ - or di- $\sigma$  binding; the differences mainly result from the extent of back-donation from the metal to the ethylene  $\pi^*$  orbital. Organometallic analogues for both types of binding exist. Zeise's salt, or K<sup>+</sup>[(C<sub>2</sub>H<sub>4</sub>)PtCl<sub>3</sub>]<sup>-</sup>, contains  $\pi$ -bound ethylene,<sup>16</sup> whereas di- $\sigma$  bonding of ethylene is found in (C<sub>2</sub>H<sub>4</sub>)Os<sub>2</sub>(CO)<sub>8</sub>.<sup>22</sup> Di- $\sigma$  bound ethylene species have been reported for several surfaces,<sup>3,5,23–28</sup> indicative of strong interactions with the metal surface. Conversely,  $\pi$ -bound complexes have been reported for surfaces where back-bonding is limited.<sup>7,29–31</sup> Many surfaces exhibit  $\pi$ -binding of ethylene with coadsorbed oxygen;<sup>3,5,27,30,32–34</sup> in such cases, electron withdrawal by the coadsorbates may limit metal electron availability to participate in back donation with the ethylene. The reactions of ethylene adsorbed on metal surfaces largely involves decomposition upon heating. Intermediates such as ethynylidyne, acetylene, vinylidene, and vinyl have all been reported to be observed in the decomposition.<sup>3,5,27,35</sup>

We report here the first studies of coadsorbed ethylene and hydrogen on Fe(100) by vibrational spectroscopy. These studies demonstrate the isolation of surface ethyl groups, formed via the migratory insertion of hydrogen into ethylene on Fe(100)–H. The reactivity of ethyl groups can thus be understood;  $\beta$ -hydride elimination of ethyl groups leads to evolution of ethylene at 225 K. Conversely, reductive elimination of the ethyl groups to evolve ethane is facilitated at 165 K by coadsorbed CO.

## Experimental Section

Experiments were performed in a stainless steel ultrahigh vacuum chamber described previously<sup>4</sup> with a base pressure of  $3 \times 10^{-11}$  Torr

(16) Powell, D. B.; Scott, J. G. V.; Sheppard, N. *Spectrochim. Acta* **1972**, *28A*, 327.

(17) Stuve, E. M.; Madix, R. J. *J. Phys. Chem.* **1985**, *89*, 3183.

(18) Bent, B. E.; Mate, C. M.; Kao, C.-T.; Slavin, A. J.; Somorjai, G. A. *J. Phys. Chem.* **1988**, *92*, 4720.

(19) Bent, B. E. Ph.D. Thesis, University of California, Berkeley, 1982.

(20) Sheppard, N. *Ann. Rev. Phys. Chem.* **1988**, *39*, 589.

(21) Herzberg, G. *Molecular Spectra and Molecular Structure II. Infrared and Raman Spectra of Polyatomic Molecules*; Van Nostrand Reinhold Company: New York, 1945.

(22) Bandy, B. J.; Chesters, M. A.; James, D. I.; McDougall, G. S.; Pemble, M. E.; Sheppard, N. *Philos. Trans. R. Soc. London Ser. A* **1986**, *318*, 141.

(23) Lehwald, S.; Ibach, H. *Surf. Sci.* **1979**, *89*, 425.

(24) Lehwald, S.; Ibach, H.; Steininger, H. *Surf. Sci.* **1982**, *117*, 342.

(25) Anson, C. E.; Bandy, B. J.; Chesters, M. A.; Keiller, B.; Oxtton, I. A.; Sheppard, N. *J. Electron. Spectrosc. Rel. Phenom.* **1983**, *29*, 315.

(26) Barteau, M. A.; Broughton, J. Q.; Menzel, D. *Appl. Surf. Sci.* **1984**, *19*, 92.

(27) Hatzikos, G. H.; Masel, R. I. *Surf. Sci.* **1987**, *185*, 479.

(28) Erley, W.; Baro, A. M.; Ibach, H. *Surf. Sci.* **1982**, *120*, 273.

(29) Nyberg, C.; Tengstal, C. G.; Andersson, S. *Chem. Phys. Lett.* **1982**, *87*, 87.

(30) Stuve, E. M.; Madix, R. J. *J. Phys. Chem.* **1985**, *89*, 105.

(31) Chesters, M. A.; McDougall, G. S.; Pemble, M. E.; Sheppard, N. *Appl. Surf. Sci.* **1985**, *22/23*, 369.

(32) Backx, C.; de Groot, C. P. M.; Biloen, P. *Appl. Surf. Sci.* **1980**, *6*, 256.

(33) Kostov, K. L.; Marinova, T. S. *Surf. Sci.* **1987**, *184*, 359.

(34) Seip, U.; Tsai, M.-C.; Kupperts, J.; Ertl, G. *Surf. Sci.* **1984**, *147*, 65.

(35) Zaera, F.; Fischer, D. A.; Carr, R. G.; Gland, J. L. *J. Chem. Phys.* **1988**, *89*, 5335.

capable of low-energy electron diffraction (LEED), Auger electron spectroscopy (AES), temperature programmed reaction spectroscopy (TPRS), and high-resolution electron energy-loss spectroscopy (HREELS) measurements. The temperature of the Fe(100) crystal, mounted on a rotatable manipulator with three degrees of freedom, could be controlled from 100 K to over 1000 K. The sample was cooled by thermal conduction from a liquid nitrogen reservoir. Resistive heating was accomplished with current flow through the tantalum support. Temperature was monitored with a chromel-alumel thermocouple spot-welded to the crystal. HREELS was conducted with a double-pass 127° cylindrical sector monochromator and a single-pass analyzer. The typical full width at half maximum (FWHM) for elastically scattered electrons was about 70 cm<sup>-1</sup>. Most gases were used as supplied from Matheson without further purification; they included argon (prepurified; 99.998% min), ethylene (C.P.; 99.5% min), hydrogen (prepurified; 99.99% min), and deuterium (C.P.; 99.7% min). Ethylene-d<sub>4</sub> (Cambridge Isotope Labs, 99% D) contained acetone impurities, which were eliminated from the sample with an ethanol/ice trap on the dosing lines. Mass spectrometer measurements assured purity of all gases admitted into the UHV system and utilized in these experiments. Dosing of hydrogen, deuterium, and ethylene was directed from capillary array dosers at close distances; the saturation exposures were easily reproduced, and chamber pressures were kept to a minimum.

Details of the preparation and initial cleaning of the Fe(100) crystal are given elsewhere.<sup>36</sup> Routine cleaning was accomplished with argon ion bombardment. First the crystal was heated to 923 K and sputtered for 10 min; the crystal was then allowed to cool to 105 K before sputtering for another 10 min. Following evacuation to 10<sup>-10</sup> Torr, the crystal was then annealed at 723 K for 5 min. AES and EELS were used to evaluate surface cleanliness. A c(2 × 2) random C<sub>a</sub> + O<sub>a</sub> overlayer resulting from the dissociation of CO<sub>a</sub><sup>37</sup> was used for AES calibration; XPS studies report dissociation of 0.24 mL of CO yield this state.<sup>38</sup> This cleaning procedure very efficiently eliminated surface carbon (0.00–0.01 mL by AES) (none detected by EELS) but was not always completely successful in removing oxygen as indicated by M–O losses<sup>39</sup> detected by EELS. Prolonged heating above 727 K brings dissolved oxygen from the Fe(100) bulk to the surface if any exists.<sup>39</sup> Excessive oxygen impurities were removed with ethylene titrations, as was necessary after exposure of the crystal to atmospheric pressures for routine maintenance or in cases where very large quantities of O<sub>a</sub> accumulated on the surface, and the routine sputtering procedure yielded little progress. However residual carbon, a product of the reaction, then needed to be sputtered away. At low concentrations O<sub>a</sub> could be titrated off at the expense of C<sub>a</sub>. With these procedures, the O<sub>a</sub> impurities could be greatly reduced (0.01–0.03 mL by AES).

All EELS spectra were recorded at 100 K following tuning of the spectrometer. Cleaning and reparation of the surface was not necessary between collection of spectra for hydrogen saturated surfaces, ethylene adsorption at 100 K, or formation of the intermediate upon annealing.

Thus, for each set of reactants, the clean surface was prepared, cooled to 100 K, saturated with hydrogen, and EELS was performed; ethylene was dosed on this surface, and the EELS spectrum was once again collected. Finally, this surface was annealed to 170 K and recooled, and the final EELS spectrum was recorded. Vibrational spectra were examined for evidence of H<sub>2</sub>O (1300 cm<sup>-1</sup>) and CO adsorption ( $\nu_{CO}$  at 1200 cm<sup>-1</sup> and/or 2000 cm<sup>-1</sup>).<sup>11</sup> Spectra recorded for the direct preparation of ethylene on Fe(100)–H and ethyl on Fe(100) (without EELS collection prior to preparation) showed no differences from the spectra recorded successively as described above.

## Results and Discussion

The EELS spectrum for a saturated hydrogen adlayer on Fe(100) is presented in Figure 1(a). Hydrogen adsorption and binding on Fe(100) has been discussed elsewhere.<sup>4</sup> Briefly, hydrogen dissociatively adsorbs on Fe(100) at 100 K binding

(36) Burke, M. L.; Madix, R. J. *Surf. Sci.* **1990**, *237*, 20.

(37) Ho, W.; Willis, R. F.; Plummer, E. W. *Phys. Rev. Lett.* **1978**, *40*, 1463.

(38) Cameron, S. D.; Dwyer, D. J. *Langmuir* **1988**, *4*, 282.

(39) Lu, J.-P.; Albert, M. R.; Bernasek, S. L. *Surf. Sci.* **1989**, *215*, 348.

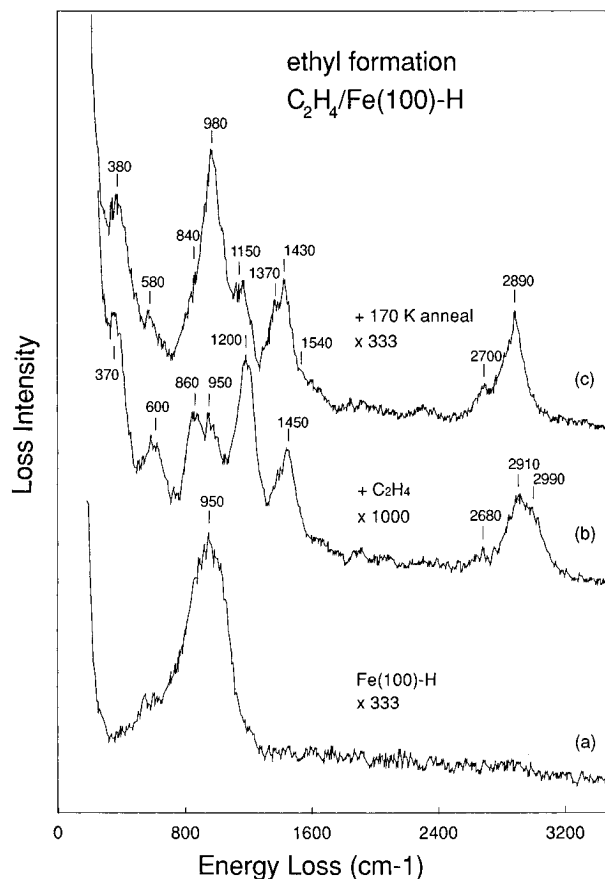


**Figure 1.** EELS: (a) saturation coverage of H<sub>(a)</sub> on Fe(100) at 100 K, (b) Fe(100)-H with saturation exposure of C<sub>2</sub>H<sub>4</sub> at 100 K, and (c) surface intermediate at 100 K following anneal to 170 K.

**Table 1.** Vibrational Assignments for Ethylene on Clean and Hydrogen-Saturated Fe(100)<sup>a</sup>

mode description	C <sub>2</sub> H <sub>4</sub> /Fe(100)-H (C <sub>2</sub> D <sub>4</sub> /Fe(100)-D)		$\nu_H/\nu_D$	C <sub>2</sub> H <sub>4</sub> /Fe(100) <sup>3</sup> (C <sub>2</sub> D <sub>4</sub> /Fe(100))		$\nu_H/\nu_D$
	$\nu$	( $\nu$ )		$\nu$	( $\nu$ )	
$\nu$ CH <sub>2(a)</sub>	2990	(2230)	1.34	2985	(2220)	1.33
$\nu$ CH <sub>2(s)</sub>	2910	(N.R.)				
$\nu$ Fe-HC	2680	(2040)	1.31	2720	(2040)	1.33
$\delta$ CH <sub>2</sub> / $\nu$ CC → ( $\delta$ CD <sub>2</sub> )	1450	(950)	1.53	1395	(900)	1.55
$\nu$ CC/ $\delta$ CH <sub>2</sub> → ( $\nu$ CC)	1200	(1270)	0.94	1095	(1160)	0.95
$\nu$ FeH	950	(700)	1.36			
CH <sub>2</sub> wag	860	(640)	1.31	860	(645)	1.33
$\nu$ FeC <sub>(s)</sub>	600	(N.R.)	560			
$\nu$ FeC <sub>(a)</sub>	370	(400)	0.93	380	(410)	0.93

<sup>a</sup> N.R. = not resolved.

within the 4-fold hollows up to a saturation coverage of 1 mL, yielding the broad peak at 950 cm<sup>-1</sup>.

Dosing C<sub>2</sub>H<sub>4</sub> upon the hydrogen-saturated surface at 100 K leads to the EELS spectrum of Figure 1(b). Assignments of the losses are summarized in Table 1. Asymmetric and symmetric CH<sub>2</sub> stretches ( $\nu$ CH<sub>2</sub>) are observed at 2990 and 2910 cm<sup>-1</sup>, respectively. Carbon-carbon stretching ( $\nu$ CC) and CH<sub>2</sub> scissors modes ( $\delta$ CH<sub>2</sub>) of the same symmetry lead to two mixed modes at 1200 and 1450 cm<sup>-1</sup>. The frequencies of the pure modes are unknown. Also observed are the CH<sub>2</sub> wag at 860 cm<sup>-1</sup> and the metal-carbon stretch ( $\nu$ FeC) at 370 cm<sup>-1</sup>. Intensity of the  $\nu$ FeH loss at 950 cm<sup>-1</sup> is greatly attenuated by coadsorbed ethylene; dipole screening is expected from the p-orbitals of ethylene. Similar attenuation was noted with the coadsorption of CO and H in a mixed adlayer.<sup>4,11</sup> A weak loss due to CH

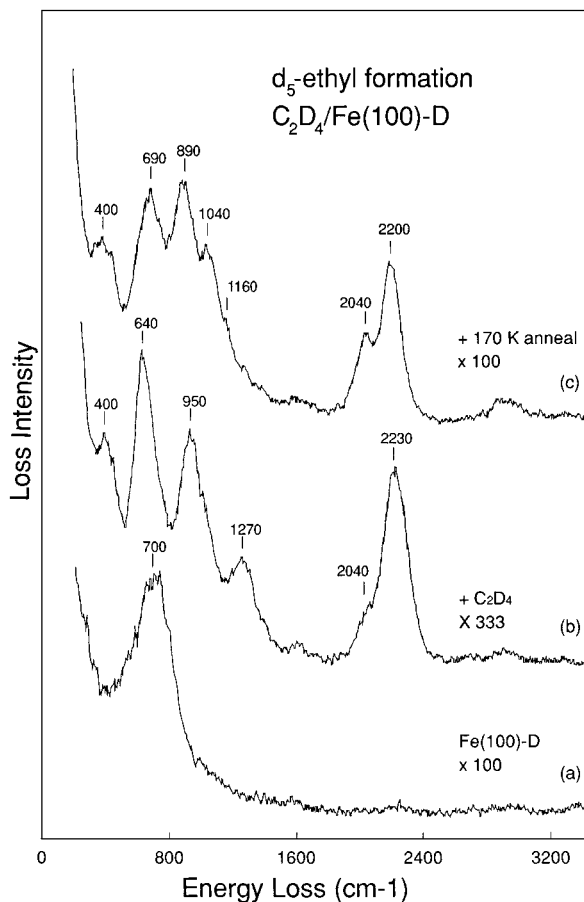


**Figure 2.** EELS: (a) saturation coverage of D<sub>(a)</sub> on Fe(100) at 100 K, (b) Fe(100)-D with saturation exposure of C<sub>2</sub>D<sub>4</sub> at 100 K, and (c) surface intermediate at 100 K following anneal to 170 K.

mode softening is observed at 2680 cm<sup>-1</sup>; such features are greatly enhanced in latter spectra and are discussed below.

Phase separation of the post-dosed ethylene and hydrogen-saturated adlayer does not occur. Hung and Bernasek have reported the EELS spectra of C<sub>2</sub>H<sub>4</sub> on clean Fe(100).<sup>3</sup> We reproduced these results in independent experiments. Comparison of Figure 1(b) with clean surface spectra demonstrate significant shifts of the ethylene vibrational modes. Table 1 includes vibrational frequencies for ethylene on clean Fe(100) for comparison.<sup>3</sup> Ethylene  $\nu$ CC and  $\delta$ CH<sub>2</sub> modes at 1095 and 1395 cm<sup>-1</sup> on the clean surface are significantly lower than values of 1200 and 1450 cm<sup>-1</sup> observed on the hydrogen presaturated Fe(100) surface. As discussed below, this redshift indicates a weakened C-C bond strength on the clean surface resulting from an increased ethylene-metal interaction. The dominance of modes different from those characteristic of adsorption on clean iron mitigates against the occurrence of phase separation.

Deuterated analogs were utilized to aid assignments of vibrational modes. Figure 2(a),(b) show deuterium on the Fe(100) surface and subsequent adsorption of C<sub>2</sub>D<sub>4</sub> at 100 K. Assignments and isotopic shifts for C<sub>2</sub>H<sub>4</sub> (C<sub>2</sub>D<sub>4</sub>) on H- (D-) saturated Fe(100) are included in Table 1 with comparison to clean Fe(100).<sup>3</sup> With these assignments, the expected<sup>40</sup> isotopic shifts,  $\nu_H/\nu_D$  are observed for the CH/CD stretching and wagging modes. Given the substantial redshift expected for the scissors mode in adsorbed C<sub>2</sub>D<sub>4</sub>, the loss at 1270 cm<sup>-1</sup> is predominantly  $\nu$ CC (although not pure), while the 950 cm<sup>-1</sup> mode is attributed to  $\delta$ CD<sub>2</sub>.

Further understanding of the  $\nu$ CC and  $\delta$ CH<sub>2</sub> modes can be gained from a consideration of the normal mode vibrations in

correlation tables of  $C_2H_4$  and *gauche*- $C_2H_4Br_2$ . Bent *et al.* have presented correlation tables for the perhydrido and perdeutero forms.<sup>18</sup> Upon bonding with a surface, the  $\nu_{CC}$  ( $A_g$ ),  $\delta_{CH_2}$  ( $A_g$ ), and  $CH_2wag$  ( $B_{1g}$ ) modes of ethylene converge to the same symmetry (A); complex mixing is expected. However, mixing of the  $\nu_{CC}$  mode is minimized considerably in the perdeutero species. Isotopic shifts of pure  $\delta_{CH_2}$  and  $\delta_{CD_2}$  modes should yield a  $\nu_H/\nu_D$  of 1.33, while the  $\nu_H/\nu_D$  of  $\nu_{CC}$  should be approximately 1.07. The highly mixed modes of perhydrido ethylene, when compared to those of perdeutero ethylene, yield *apparent*  $\nu_H/\nu_D$  values which differ from those expected; deviations from these values result from mixing of the pure modes in the perhydrido species, which is reduced upon isotopic substitution. Using the correlation tables of Bent *et al.*, the 1270  $cm^{-1}$  loss for  $C_2D_4$  on the deuterium-presaturated surface would suggest that in the perhydrido species, the “pure”  $\delta_{CH_2}$  and  $\nu_{CC}$  modes can be expected near 1325  $cm^{-1}$  (the midpoint of the observed bands).

Since determination of  $\nu_{CC}$  for ethylene is complicated by mixing with the  $\delta_{CH_2}$  mode of similar symmetry, Stuve and Madix have proposed a  $\pi\sigma$  parameter as a measure of rehybridization which combines the percentage shift to lower frequency of both the  $\delta_{CH_2}$  and  $\nu_{CC}$  modes upon adsorption.<sup>17</sup> The parameter is normalized to zero for gas-phase ethylene and unity for 1,2-dibromoethane, which represent the extremes of rehybridization. The organometallic compound  $K[(C_2H_4)PtCl_3]$ <sup>16</sup> (Zeise’s salt), in which ethylene is bound with intermediate rehybridization to the Pt atom ( $\pi$ -bonding),<sup>41</sup> exhibits a  $\pi\sigma$  parameter of 0.38 (0.35 for deuterated Zeise’s salt).  $C_2H_4$  adsorption on Pt(111) shows the largest rehybridization on surfaces with  $\pi\sigma$  parameter of 0.92 (0.88) and can be characterized as di- $\sigma$  bonding. Very weakly bound and weakly rehybridized species exist in complexes such as  $Ag(C_2H_4)BF_4$ ,<sup>16</sup> ( $\pi\sigma = 0.12$ ), and on surfaces such as oxygen-precovered  $Ag(110)$ <sup>32</sup> ( $\pi\sigma$  parameter = 0.14).

Bent *et al.* have suggested that the deuterated  $\pi\sigma$  parameter is the more reliable measure of rehybridization,<sup>18</sup> since the  $\nu_{CC}$  is less coupled with the  $\delta_{CD_2}$  mode, thus yielding a parameter more simply related to the extent of rehybridization. The  $\pi\sigma$  parameter for deuterated species scales from 0 to 0.78 (not unity); however there is only good agreement between the perhydrido- and perdeutero-  $\pi\sigma$  parameters up to 0.4. Therefore, for ease of comparison between perhydrido and perdeutero ethylene, especially with highly rehybridized species, Bent *et al.*, propose the application of a DCD parameter which considers only the  $\nu_{CC}$  for deuterated ethylene complexes.<sup>19</sup> This should be the only mode in the 1100 to 1550  $cm^{-1}$  range and be relatively free of coupling with the  $\delta_{CD_2}$  mode. The DCD parameter scales from 0 to 1 throughout the entire rehybridization range of  $C_2D_4$  complexes.

Table 2 presents  $\pi\sigma$  and DCD parameters for ethylene on several transition metal surfaces in comparison to  $C_2H_{4(g)}$ ,  $C_2H_4Br_{2(g)}$ , and Zeise’s salt. Based on our results, ethylene adsorption at 100 K on Fe(100)-H exhibits  $\pi\sigma$  parameters of 0.58 (0.53) and a DCD parameter of 0.66. EELS data for  $C_2H_4$  and  $C_2D_4$  on the clean Fe(100) surface yield  $\pi\sigma$  parameters of 0.89 (0.86) and a DCD of 0.95.<sup>3</sup> These results indicate that ethylene is less strongly rehybridized on the hydrogen-presaturated Fe(100) surface than on the clean surface. Hydrogen presaturation of

**Table 2.** Extent of Rehybridization as Indicated by  $\pi\sigma$  and DCD Parameters

species/substrate	$\pi\sigma$ $C_2H_4$ ( $C_2D_4$ )		DCD
$C_2H_{4(g)}$ <sup>44</sup>	0	(0)	0
Cu(100) <sup>29</sup>	0.21	(0.27)	0.25
Pd(110) <sup>31</sup>	0.38	(0.38)	0.38
zeise’s salt <sup>16</sup>	0.38	(0.35)	0.43
Fe(100)-H	0.58	(0.53)	0.66
Ru(001) <sup>26</sup>	0.85	(0.78)	0.8
Fe(100) <sup>3</sup>	0.89	(0.86)	0.95
Pt(111) <sup>5</sup>	0.92	(0.85)	0.96
$C_2H_4Br_{2(g)}$ <sup>44</sup>	1.00	(0.78)	1

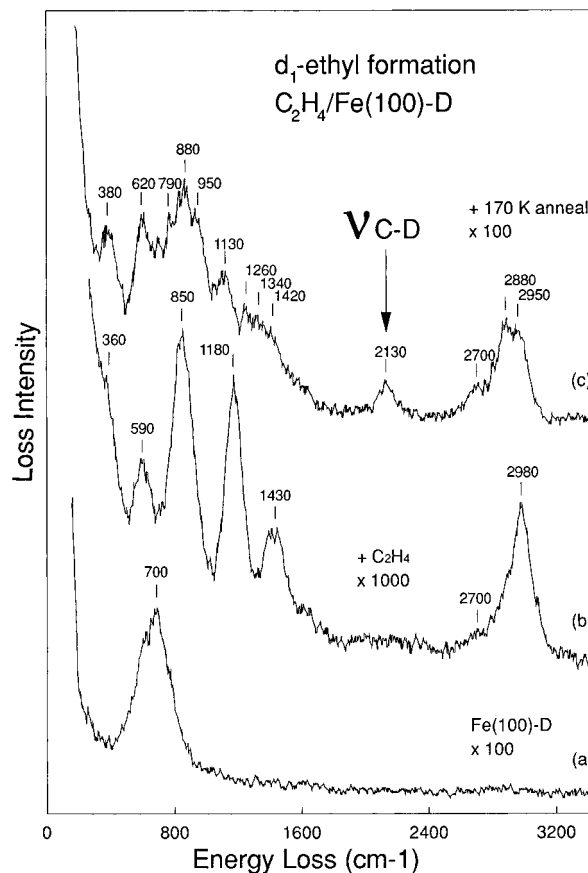


**Figure 3.** EELS: (a) saturation coverage of D<sub>(a)</sub> on Fe(100) at 100 K, (b) Fe(100)-D with saturation exposure of  $C_2H_4$  at 100 K, and (c) surface intermediate at 100 K following anneal to 170 K.

the surface appears to reduce back donation from metal orbitals into the  $\pi^*$  orbitals of ethylene compared to the bonding of ethylene on the clean surface. This result is consistent with the reactivity of  $C_2H_4$  on the different iron surfaces. Ethylene decomposes on all low index clean iron surfaces, (100), (110), and (111),<sup>3,28,34</sup> whereas the Fe(100)-H surface affects no decomposition.

EELS spectra for the intermediate formed and isolated by annealing  $C_2H_4$  ( $C_2D_4$ ) on the H (D) presaturated Fe(100) surface to 170 K are presented in Figures 1(c) and 2(c). As previously noted, formation of such an intermediate was indicated by previous TPRS experiments,<sup>1</sup> which were reproduced here. Comparison of these vibrational spectra with Figures 1(b) and 2(b) clearly indicate an intermediate different from the  $\pi$ -bonded ethylene.

Mixed isotope experiments with  $C_2H_4$  adsorption on Fe(100)-D were performed. Figure 3 shows the EELS spectra for adsorption at 100 K followed by annealing to 170 K. The anneal leads only to evolution of pure  $C_2H_4$  into the gas phase

(40) Lowry, T. H.; Richardson, K. S. *Mechanism and theory in organic chemistry*, 2nd ed.; Harper & Row: New York, 1981.

(41) Molecular calculations of electron density in ethylene  $\pi$  and  $\pi^*$  orbitals demonstrate limited, but finite back-bonding in Zeise’s salt.<sup>15</sup> Thus, as a model of  $\pi$  bonding, Zeise’s salt represents the organometallic analog with *weak* back-bonding; however, it is not an example of *pure*  $\pi$  bonding.

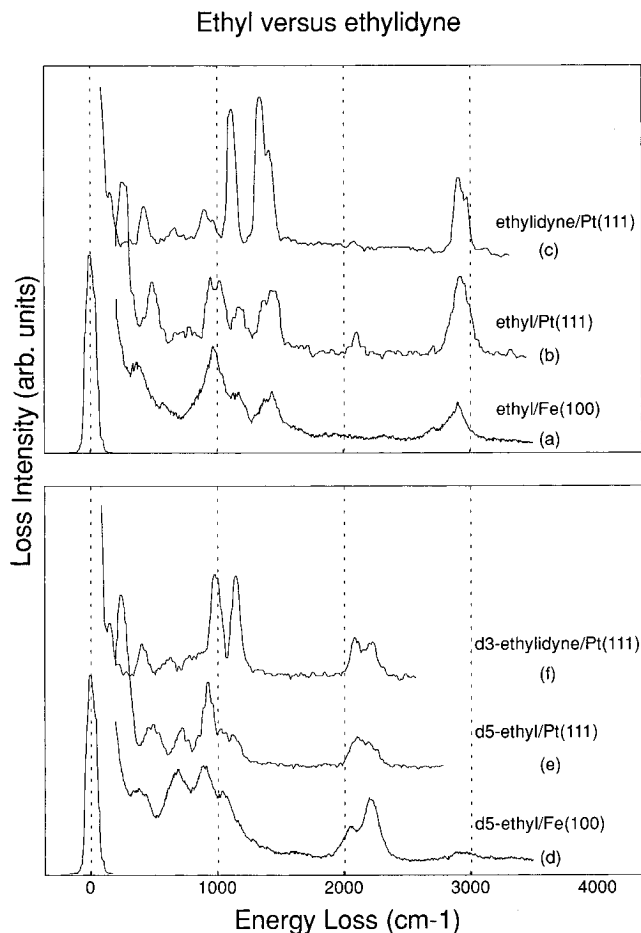


**Figure 4.** EELS: comparison of perhydrido- and perdeutero- ethyl intermediates formed on Fe(100) with ethyl[42] and ethylidyne[5] species isolated on Pt(111); (a) ethyl/Fe(100)-H, (b) ethyl/Pt(111), (c) ethylidyne/Pt(111), (d) ethyl-*d*<sub>5</sub>/Fe(100), (e) ethyl-*d*<sub>5</sub>/Pt(111), (f) ethylidyne-*d*<sub>3</sub>/Pt(111).

at 170 K—no deuterated species evolved. Upon further heating of the intermediate, ethylene-*d*<sub>1</sub> is evolved at 225 K. Observation of  $\nu$ CD at 2130  $\text{cm}^{-1}$  following the anneal to 170 K clearly indicates the formation of C-D bonds (Figure 3(c)). No such features were observed in Figure 3(b), indicating formation of the intermediate occurs above the adsorption temperature of 100 K and below 170 K.

The vibrational spectra of Figures 1(c), 2(c), and 3(c) mitigate against ethylidyne (CCH<sub>3</sub>) as the intermediate. Ethylidyne intermediates have been isolated on Ru(001),<sup>9</sup> Rh(111),<sup>6</sup> Pd(111),<sup>7</sup> Ir(111),<sup>8</sup> and Pt(111).<sup>5</sup> Spectra in all cases are characterized by a pair of very intense modes ( $\nu$ CC and  $\delta$ CH<sub>3</sub>) between 1000 and 1400  $\text{cm}^{-1}$  which dominate the spectral region at frequencies below the  $\nu$ CH<sub>3</sub> modes. The vibrational spectrum of the intermediate on hydrogen-saturated Fe(100) is inconsistent with ethylidyne; losses below 1000  $\text{cm}^{-1}$  dominate. Figure 4 shows the vibrational spectra for perhydrido- and perdeutero-ethylidyne and ethyl groups on Pt(111)<sup>5,42,43</sup> along with the spectra of Figures 1(c) and 2(c). The similarity of these spectra strongly suggest that the intermediate produced by the 170 K anneal is surface-bound ethyl.

Vibrational assignments for the ethyl intermediate on Fe(100)-H are presented in Table 3 with comparison to analogous ethyl species on Pt(111)<sup>42</sup> and gas phase C<sub>2</sub>H<sub>5</sub>Cl<sub>(g)</sub>.<sup>44</sup> As expected, the ethyl groups exhibit a significantly reduced  $\nu$ CC frequency at 980  $\text{cm}^{-1}$ . Other prevalent modes include CH

(42) Lloyd, K. G.; Roop, B.; Campion, A.; White, J. M. *Surf. Sci.* **1989**, 214, 227.

**Table 3.** Vibrational Assignments for Ethyl on Fe(100)-H with Comparison to C<sub>2</sub>H<sub>5</sub>Cl<sub>(g)</sub><sup>44</sup> and Ethyl on Pt(111)<sup>42 a</sup>

mode	C <sub>2</sub> H <sub>5</sub> / Fe	C <sub>2</sub> D <sub>5</sub> / Fe	$\nu_{\text{H}}/\nu_{\text{D}}$	C <sub>2</sub> H <sub>5</sub> Cl <sub>(g)</sub>	C <sub>2</sub> H <sub>5</sub> / Pt	C <sub>2</sub> D <sub>5</sub> / Pt	$\nu_{\text{H}}/\nu_{\text{D}}$
$\nu$ CH <sub>2(s)</sub>				2967		2205	1.32
$\nu$ CH <sub>3(a)</sub>	2890	2200	1.31	2946	2918	2264	1.29
$\nu$ CH <sub>3(s)</sub>				2881		2154	1.35
$\nu$ Fe-HC	2700	2040	1.32				
CH <sub>2</sub> sciss	1540	1160	1.33	1448	1450	1130	1.28
CH <sub>3</sub> def <sub>(a)</sub>	1430	1040	1.38	1448	1430	1071	1.34
CH <sub>3</sub> def <sub>(s)</sub>	1370			1385	1376	1024	1.34
CH <sub>2</sub> wag	1150	890	1.29	1289	1173	929	1.26
$\nu$ CC	980	890	1.10	974	1022	929	1.10
CH <sub>2</sub> twist				1251	894		
CH <sub>3</sub> rock	840	690	1.22	974	941	729	1.29
$\nu$ MC	380	400	0.95		484	480	1.01
$\nu$ PtCl					252	248	

<sup>a</sup> Contributions to the vibrational spectra of Figures 1(c) and 2(c) also arise from coadsorbed hydrogen ( $\nu$ FeH = 950  $\text{cm}^{-1}$ ) and deuterium ( $\nu$ FeD = 700  $\text{cm}^{-1}$ ).

stretching at 2890  $\text{cm}^{-1}$ , CH<sub>3</sub> deformation at 1430  $\text{cm}^{-1}$ , CH<sub>2</sub> wagging at 1150  $\text{cm}^{-1}$ , and CH<sub>3</sub> rocking near 840  $\text{cm}^{-1}$ . The 980  $\text{cm}^{-1}$  loss of Figure 1(c) is intensified by poor resolution between the  $\nu$ CC,  $\nu$ FeH, and CH<sub>3</sub> rocking modes on the hydrogen-covered surface. The spectrum of Figure 2(c) exhibits increased intensity in two modes due to overlap of the CD<sub>3</sub> rock and  $\nu$ FeD and overlap of  $\nu$ CC and CD<sub>2</sub> wag modes. Hydrogenic modes exhibit the expected isotopic shifts. Excellent agreement with C<sub>2</sub>H<sub>5</sub>Cl<sub>(g)</sub> and ethyl/Pt(111) are indicated by Figure 4 and Table 3.

Assignment of the losses in Figure 3(c) is complicated by isotopic effects resulting from insertion of a single D atom into the C<sub>2</sub>H<sub>4(a)</sub> species. The aforementioned 2130  $\text{cm}^{-1}$  loss is attributed to CD stretching in the methyl end of the ethyl-*d*<sub>1</sub> intermediate. Loss of symmetry affects the CH<sub>3</sub> deformation (near 1340  $\text{cm}^{-1}$ ) and the CH<sub>3</sub> rock (near 880  $\text{cm}^{-1}$ ). The CH<sub>2</sub> wag appears relatively unperturbed at 1130  $\text{cm}^{-1}$ . CH stretching modes are still prevalent in the ethyl-*d*<sub>1</sub> species as evidenced by  $\nu$ CH<sub>2</sub> at 2880  $\text{cm}^{-1}$  and  $\nu$ CH<sub>2</sub>D at 2950  $\text{cm}^{-1}$ .

The ethyl groups on Fe(100)-H exhibit softened CH(CD) modes at 2700  $\text{cm}^{-1}$  (2040  $\text{cm}^{-1}$ ). The frequencies of these features are too low to be attributed to symmetric CH stretches. Unusually low frequency (softened) C-H vibrational modes have been reported for several hydrocarbons on transition metal surfaces. For example, cyclohexane demonstrates significantly lowered CH stretching frequencies on Ru(001) (404  $\text{cm}^{-1}$ ),<sup>45</sup> Pt(111) (310  $\text{cm}^{-1}$ ),<sup>46</sup> and Ni(111) (180  $\text{cm}^{-1}$ ),<sup>46</sup> softened C-H and C-D stretches have been observed for methyl on Ni(111)<sup>47</sup> and Cu(111)<sup>48</sup> and for ethyl and propyl on Cu(111).<sup>48</sup>

Many examples exist in organometallic clusters where C-H groups interact with the metal via a two-electron three-center, "agostic" bond, producing a marked effect on molecular and electronic structure and thus on the reactivity of the molecule.<sup>49</sup> Several relevant examples of such bonds exist, including methyl and ethyl hydrogens, and iron centers are prevalent in this body of work. This bonding can occur by donation of electrons from

(43) Thermal treatment of ethylene on clean Pt(111) leads to the formation and isolation of ethylidyne,<sup>5</sup> whereas photolysis of C<sub>2</sub>H<sub>5</sub>Cl<sub>(a)</sub> produces ethyl intermediates coadsorbed with Cl<sub>(a)</sub>.<sup>42</sup>

(44) Shimanouchi, T. *Tables of Molecular Vibrational Frequencies Consolidated Volume I*; U.S. Dept. of Commerce, NSRDS-NBS, 1972.

(45) Hoffmann, F. M.; Felner, T. E.; Thiel, P. A.; Weinberg, W. H. *Surf. Sci.* **1983**, 130, 173.

(46) Demuth, J. E.; Ibach, H.; Lehwald, S. *Phys. Rev. Lett.* **1978**, 40, 1044.

(47) Yang, Q. Y.; Maynard, K. J.; Johnson, A. D.; Ceyer, S. T. *J. Chem. Phys.* **1995**, 102, 7734.

(48) Lin, J.-L.; Bent, B. E. *Chem. Phys. Lett.* **1992**, 194, 208.

(49) Brookhart, M.; Green, M. L. H. *J. Org. Chem.* **1983**, 250, 395.

C–H bonding orbitals to the metal or by donation of electron density from the metal to antibonding C–H orbitals. With these species, the C–H–M bond contributes to satisfying the valence of the metal center, thus stabilizing the complex. In our case, available interactive sites may be made available by the hydrogen atoms that add to ethylene to form ethyl. However, electronic structure calculations and the vibrational information we have obtained cast doubt on such an interpretation, at least to the extent that this bonding contributes to the reactivity of the adsorbed ethyl group.

Yang and Whitten<sup>51</sup> find that methyl groups in their lowest energy configuration exhibit no sign of metal–hydrogen bonding interactions, and, indeed, *repulsive* interactions were found between hydrogen and nickel. Lowering of C–H stretching frequencies was observed when the methyl group was moved to an asymmetric binding site and the methyl group was tilted so that one of the hydrogen atoms resided above one nickel atom; the energetic cost of this displacement was 1.6 kcal/mol. In this configuration there was a net charge gain on all three hydrogens as well as on the nickel atom below the hydrogen and a net charge loss on the carbon atom. For Ti(0001), Cr(110), and Co(0001) Zheng et al.<sup>51</sup> found the M–H interactions with adsorbed methyl to be slightly antibonding in the energetically favorable atop sites, but weak M–H interactions were reported for bonding of the methyl group in the 3-fold hollow. Hoffmann et al.<sup>52</sup> explain mode softening in cyclic hydrocarbons on Ru(001) in terms of proximity of the hydrogen with the surface; however, their electronic structure calculations indicated the origin of the frequency shift is not attractive interactions between the hydrogen and metal atoms (hydrogen bonding) but rather Pauli exchange repulsions that increase as the CH bond approaches the surface in the most stable bonding geometry of the ligand. These repulsions tend to increase the CH bond length and thus manifest themselves in decreased stretching frequencies. Similarly, Schüle et al. report reduction of the C–H stretching frequencies for methyl on Ni(111) in the lowest energy binding site (3-fold hollow) and attribute this effect to charge donation from the metal into the C–H antibonding molecular orbitals.<sup>53</sup> It is noteworthy, however, that they state that their results are in agreement with Hoffmann et al. and that this interaction is *not* a precursor to dehydrogenation. To test the relationship between C–H bond softening and the presence of H-bonding to the surface, Hoffmann et al. determined the binding energies of several C<sub>n</sub>H<sub>2n</sub> (*n* = 3–6, 8) cyclic hydrocarbons on Ru(001); they found no correlation between the surface-molecule binding energies and the appearance of mode softening; i.e., in this case there appear to be no “H-bonding” interactions with the surface, even though the vibrational frequencies are lowered.<sup>52</sup> Raval and Chesters, on the contrary, suggest that there is a significant correlation between C–H bond softening and either the surface binding energy or the propensity for dehydrogenation in adsorbed cyclohexane on metal surfaces.<sup>54</sup>

It is indeed tempting to associate the  $\beta$ -H elimination from ethyl on Fe(100)–H with the mode softening observed in this work. However, the EELS spectra indicate that the mode softening is associated with the  $\alpha$ -carbon, not the  $\beta$ -carbon, of

the ethyl group. When adsorbed ethyl is formed by reaction of preadsorbed deuterium with perhydrido ethylene, the deuterium is expected to reside in the methyl group. In that case (Figure 3) there is no sign of C–D bond softening. For comparison, the isolated C–D stretching frequency in singly deuterated, adsorbed methoxy on Ni(100) is 2152 cm<sup>-1</sup>.<sup>55</sup> This behavior is identical to that observed for ethyl groups on copper for which mode softening occurs at the  $\alpha$ -carbon, even though this species reacts by  $\beta$ -elimination.<sup>48</sup> In that case mode softening is attributed to charge donation from the metal into the C–H antibonding orbitals; a similar explanation of the C–H bond softening in methyl on Ni(111) has been offered.<sup>47</sup> However, these interpretations are based on the recent electronic structure calculations discussed above, and there seems to be some ambiguity in the theoretical interpretations. Most importantly, however, the mode softening we observe appears not to be associated with the  $\beta$ -elimination reaction on Fe(100)–H.

If this reduction in frequency is associated with C–H bond weakening, it is notable that it does not produce reaction by  $\alpha$ -elimination. It could of course be argued that  $\alpha$ -elimination would lead to decomposition of the ethyl group to carbon and hydrogen, but, when heated, the only species which desorb that desorb from the mixed layer of ethyl groups and hydrogen are ethylene and hydrogen, and no detectable carbon accumulates on the surface. Thus, if this mode softening is the result of weakening of the C–H bond by a type of “agostic” bonding, the transition state for  $\alpha$  C–H bond rupture must still lie energetically above that for  $\beta$ -elimination. Alternatively, the explanation of Hoffman et al. may account for the mode softening, and there may be no weakening of the C–H bond. At this time this issue cannot be resolved.

In summary, the identification of the ethyl intermediate is based on the nearly identical spectra of Figure 4(parts a-b and d-e) in conjunction with the chemical evidence obtained in previous work.<sup>1</sup> Specifically, the vibrational spectra reported here are consistent with ethyl groups and inconsistent with the vibrational spectra reported for ethylidyne. Further, incorporation of deuterium in the intermediate is clearly revealed in mixed isotope experiments. All vibrational losses for the intermediate isolated upon heating ethylene on the hydrogen- presaturated Fe(100) surface are assigned to vibrational modes of surface ethyl groups, and isotopic shifts for the perdeutero ethyl species are consistent with these assignments. Such vibrational modes cannot arise from surface ethylidyne.

## Conclusions

Hydrogen preadsorbed on Fe(100) limits the extent of electron back-donation to ethylene, resulting in rehybridization intermediate between the gas phase species (sp<sup>2</sup>) and the di- $\sigma$  bonded species adsorbed on the clean Fe(100) surface. Insertion of coadsorbed hydrogen occurs into adsorbed ethylene, leading to the formation of ethyl groups on Fe(100)–H. Upon heating the ethyl,  $\beta$ -hydride elimination occurs at 225 K to evolve ethylene, whereas coadsorbed CO facilitates reductive elimination at 170 K to evolve ethane.

**Acknowledgment.** The authors gratefully acknowledge the support of the National Science Foundation (NSF CHE 89-19406-A1) without which this work would not have been possible.

JA953484L

(55) Huberty, J.; Madix, R. J. *Surf. Sci.*, in press.

(50) Yang, H.; Whitten, J. L. *J. Am. Chem. Soc.* **1991**, *113*, 6442.

(51) Zheng, C.; Apeliog, Y.; Hoffmann, R. *J. Am. Chem. Soc.* **1988**, *110*, 749.

(52) Hoffmann, F. M.; Upton, T. H. *J. Phys. Chem.* **1984**, *88*, 6209.

(53) Schüle, J.; Siegbahn, P.; Wahlgren, U. *J. Chem. Phys.* **1988**, *89*, 6982.

(54) Raval, R.; Chesters, M. A. *Surf. Sci.* **1988**, *219*, L505.